WIND EFFECTS ON TILED ROOFS—WIND SAFETY AND VENTILATION

C. KRAMER and H.J. GERHARDT
WSP Consulting Engineers
Aachen, Germany

This paper describes the wind load mechanism for tiled roofs. Results of extensive wind tunnel studies concerning the wind pressure distribution on pitched roofs and around individual tiles are presented. The influence of the tile design (e.g., leading edge radius, permeability of overlap) and the use of an underlay on the batten space pressure, and therefore on the net wind loads for common tile shapes, are given. The performance of special nails to increase the wind safety is also discussed.

Attics are increasingly converted to living spaces. To decrease thermal losses, insulation is often fitted between the rafters. To avoid moisture accumulation due to condensation problems the remaining batten space has to be vented. Ridge vents are commonly used in combination with openings near the eave. The paper presents results of a comprehensive study to evaluate the venting performance of typical ridge vents.

KEYWORDS

Batten space venting, pitched roofs, ridge vents, snow penetration, tiles and slates, wind load.

INTRODUCTION

Wind loading data available for building surfaces are usually based on wind tunnel tests with simple building models having smooth and wind impermeable surfaces. In Europe, however, most pitched roofs are covered with tiles as outer, weather-protecting surfaces. The wind load on the surface elements, such as tiles or slates, corresponds to the difference of external pressure and underelement pressure. The latter depends on the external pressure distribution of the roof, the wind permeability of the surface and on the possibility of pressure equilibration underneath the permeable surface. Therefore, the element wind load may differ significantly from the load derived from the external pressure distribution alone.

Pitched roofs are increasingly fitted with thermal insulation. Due to ease of installation, the insulation material is normally fitted between the rafters. An underlay is then spanned across the rafters, leaving an air space between the thermal insulation layer and underlay, and between underlay and tiled surface. To prevent moisture accumulation the air space must be vented sufficiently. The necessary venting may be achieved easily by using efficient ridge vents in combination with appropriate openings underneath the eaves.

This paper gives the description of the wind pressure field on pitched roofs and of the wind loading mechanism for wind permeable surfaces. Typical test results for roof tiles are presented. Furthermore, the airflow mechanism for vented pitched roofs will be discussed and the venting performance for typical roof vents will be addressed.

WIND LOADING MECHANISM FOR TILED ROOF SURFACES

The wind load acting on an element of a wind permeable roof surface is due to the difference of the pressures on the upper side and the bottom side of the element surface.[1] The external pressure distribution depends on the building flow field and the local element flow field. The internal pressure is governed by the external pressure and by the pressure equilibration process through the surface permeability and along the air space between tiled surface and wind impermeable layer (underlay or building wall). The former process leads to what may be termed as "tile resistance," the latter one leads to an underelement resistance. Large permeabilities will lead to low tile resistance and large batten spaces to low underelement resistance. There are two limiting cases of practical importance.[2] (1) Pavers or insulation boards put on a flat and smooth roof surface will have very high underelement resistance and relatively small tile resistance.[3] (2) Tiled surfaces on pitched roofs will experience relatively large tile resistance and very low underelement resistance.

In case (1), the underelement pressure distribution will be similar to the external pressure distribution, thus leading to relatively small net wind loads. In case (2), the underelement pressure will be nearly constant. The net wind load for single tiles will be relatively large in the wind critical areas of high external suction. Figure 1 gives a schematic drawing of the two limiting cases considered. Whereas for the case of pavers or insulation boards the external flow field is not influenced by the pavers due to their smooth upper surface, the external pressures acting on tiles (in a zone of attached flow) consist of a superposition of the pressure distributions due to the building flow field and due to the element flow field.

The local flow field is important for the wind safety of tiles and slates. For the situation considered in Figure 1, the stagnation zones at the overlapping gaps will lead to relatively large internal pressures. In addition, the flow acceleration around the windward edges of the tiles leads to a suction peak resulting in a strong tilting moment. It should be noted that fundamental aerodynamic considerations concerning optimum tile shapes may lead to an increase in wind safety of tiled roof surfaces (see "Methods to Improve the Wind Safety of Tiled Surfaces").

WIND LOAD ON TILED PITCHED ROOF SURFACES

Pressure Distribution on Pitched Roofs

Wind loading codes and standards provide information concerning time averaged pressures on flat and pitched roofs. Usually, the design pressure coefficients given depend only on the roof pitch angle. The influence of the varying flow displacement due to different relative building dimensions

is usually not considered. In an early parametric study Chien et al[4] measured the pressure distribution on flat and pitched roofs for various length/width (l/w) and height/width (h/w) ratios. The investigation was conducted in smooth wind tunnel flow. However, the results of Chien et al are in agreement with pressure measurements of the authors conducted in a wind flow corresponding to open country exposure.[6-8] Some results of the tests conducted by the authors are presented in Figure 2. For low pitched roofs ($\Theta = 15°$) the highest external suction occurs for yawing flow, $\alpha = 45°$. The pressure distribution on the windward side of the roof corresponds to the well-known pressure distribution on a flat roof with conical vortices centered at the windward corner. Time averaged, local pressure coefficients may be as high as $c_p = -4$. The conical vortices will decrease in strength with increasing roof pitch angle. For medium pitched roofs ($\Theta = 30°$), the critical flow situation occurs for wind direction perpendicular to the ridge ($\alpha = 0°$). A vortex with its axis parallel to the ridge is formed leading to a zone of high negative pressure underneath the separation bubble. Pressure coefficients for major parts of the roof may reach values of $c_p = -1.2$. The flow reattaches near the ridge. Typical time averaged pressure coefficients for the ridge area are $c_p = -0.5$. Though the negative pressures are higher near the eaves as compared to the ridge area, the critical uplift area is near the ridge. Here the element flow field superimposed on the building flow field leads to critical loadings (see "Failure Mechanism of Tiled Roofs").

For coding purposes, the pressure distributions measured in wind tunnel tests have to be simplified. Usually, the roof area is divided into three regions;[5,9] corner region, edge region and middle region (see Figure 3). For each region, the time averaged pressure coefficient is assumed to be constant. The influence of the building geometry is taken into account by the parameters relative length l/w and relative height h/w. It should be noted that for low pitched roofs the pressure coefficients in the edge and middle regions may be significantly higher than for flat roofs.

Net Wind Load

As stated above, the net wind load acting on a tile corresponds to the difference between external and underelement pressure. The underelement pressure for a tiled roof is the batten space pressure. The external pressure on roofs as given in codes of practice and standards is representative for the external local wind load on a tiled roof only if the flow is not attached to the roof. For regions, where the wind flow is attached to the roof surface, the element flow field may alter the local flow field on a roof significantly. A typical result of a detailed study by the authors is given in Figure 4. A section of a typical covering for pitched roofs was fitted to the floor of the wind tunnel test section. The test specimen included rafters, battens and tiles. The test section floor may be considered as a wind impermeable underlay or a wind impermeable thermal insulation layer. The test section roof was adjusted to produce a longitudinal pressure gradient typical for the ridge region of a steep roof (Θ 40°) and wind direction perpendicular to the ridge. Figure 4 gives the distribution of the external pressure due to the building flow field ($c_{p\,ex}$) to which the local pressure distribution due to the element flow field ($c_{p\,tile}$) is superimposed. As expected, the batten space pressure ($c_{p\,int}$) is uniform. For the case considered, the underelement flow resistance is much smaller than the tile flow resistance (see "Pressure Distribution on Pitched Roofs"). It is important to note that the batten space pressure is less negative than the average value of the external pressure distribution. This is due to the fact that the predominant permeability of the tiled surface is situated in the stagnation area of the overlap region. In fact, the batten space pressure agrees quite well with the static pressure near the overlaps.

The batten space pressure is determined by the permeability of the tiled surface. The permeability may be specified by a nondimensional permeability factor C_D.[5] The permeability factor is a function of the percentage open area (see Figure 5). Large C_D is equivalent to small permeabilities and vice versa. In general, concrete tiles have—due to their small manufacturing tolerances—a smaller permeability than clay tiles. In comparison, wind permeable facade elements cover a much wider range of permeabilities.[2]

The authors derived a simple model to calculate the batten space pressure corresponding to given external pressure distributions, if the element flow field is neglected. The calculation neglects the influence of the tile shape on the external pressures. The basis for the calculation is the continuity equation, i.e., the volume flow in the batten space and the volume flow discharged to the tiled surface have to be the same. The external pressure distribution is described by a quadratic function. The resulting integral equation can be solved.[7] (Figure 6 shows an example.) The calculated batten space pressure p_{int} is approximately 10 percent below the area averaged pressure $\overline{p_{int}}$. Thus, the batten space pressure is close to the area averaged external pressure.

A significant effect on the batten space pressure is, however, due to the change of the building flow field by the element flow field. This effect is most pronounced for flow direction perpendicular to the ridge, since the surface flow field is stagnated at the overlaps of the tiles. For sufficient permeability of the overlap gaps, this flow direction will lead to a remarkable increase in batten space pressure.

Figure 7 shows the element pressure distribution for a concrete tile widely used in Germany for different wind directions. For flow towards the overlap gaps, a suction peak occurs at the leading edge of the tiles. This peak is most pronounced for flow perpendicular to the ridge. The suction peak, which leads to a large tilting moment around the pivoting line, may be decreased by increasing the edge curvature radius (see Figure 8). Such an "aerodynamically optimized" tile has been introduced by a large German tile manufacturer.

Failure Mechanism of Tiled Roofs

Hazelwood[9] showed that roof failure on tiled surfaces occurs due to a moment turning the tile upward around the pivoting line on the batten. The turning moment consists of a lifting force and two force couples caused by the external and internal pressure distributions, respectively. This failure mechanism could be observed in wind tunnel tests. Figure 9 shows a short sequence of a movie film taken during typical tests.

The largest component of the tilting moment is caused by the external pressure distribution, when large suction peaks occur at the leading edge. As may be seen from Figure 7, suction peaks at the leading edge occur only for flow directions more or less perpendicular to the ridge. To lift tiles up sufficiently for failure to occur, the local velocities must

be relatively high. Fortunately, high local velocities perpendicular or nearly perpendicular to the ridge occur only in small areas of a pitched roof. From flow visualization studies, those areas have been identified and are depicted in Figure 10. The size and the position of the critical areas depend on the roof pitch angle.

Methods to Improve the Wind Safety of Tiled Surfaces

The most common methods claimed to improve the wind safety of tiled roofs are:

- Nails or clamps.
- Using an underlay.
- Aerodynamically favorable tile shapes.

The authors have investigated a great number of nails and clamps. Almost all types investigated may be classified as either easy to fit and being of little use, or difficult to handle but improving the wind safety. Figure 11 gives typical results for a concrete tile widely used in Germany with two common clamps. The speed of the undisturbed flow at eave height, for which failure occurred, is plotted versus roof pitch angle. Only clamp B increases the wind safety noticeably. Also included in Figure 11 is the design wind speed according to the German Standard DIN 1055 Part 4 for building heights 8m and 20m, respectively.

An underlay sealing the batten space against the space underneath the roof will not prevent cladding elements on the windward roof from being lifted up. Due to the sealing effect of the underlay, the windward side of the batten space is now mainly subjected to the high pressures at the stagnation zones in the overlap regions. Thus, an underlay may in fact increase the batten space pressure on the windward side, and therefore lead to a decrease in wind safety. However, the pressure equilibration in the gable room is prevented, leading to a much lower net wind load for the leeward roof tiles.

As pointed out above and shown in Figure 8, aerodynamically shaped tiles will prevent the large suction peak at the leading edges. In addition, the permeability at the interlocking gaps perpendicular to the ridge, where suction due to the element flow field occurs (see Figure 7), should be high, at least somewhat higher than the permeability of the overlap gap. This will lead to a decrease in batten space pressure resulting in an improved wind safety.

BATTEN SPACE VENTING

Venting of the batten space may be another means to decrease the underelement pressure. However, it is usually incorporated in thermally insulated roof systems to avoid accumulation of condensed moisture in the insulation layer. For this purpose, a sufficient air flow in the batten space is necessary since the moisture has to be accommodated by a relatively small air volume.

Venting Mechanism

Figure 12 shows a cross section of a typical roof system with thermal insulation between the rafters. The space between the underlay—if fitted—and the thermal insulation layer has to be vented. The aerodynamic situation is comparable to the flow through a duct with a height corresponding to the gap height, and a width corresponding to the distance between the rafters. The duct has an inlet opening at the eaves and an exit opening at the ridge. It may be shown[10,11] that for venting gap heights of s ◄ 20mm, the frictional losses will dominate the total pressure losses (Figure 13). The total pressure loss and the pressure loss due to friction are plotted versus the gap height s for a volume flow of $V = 4 \times 10^{-3}$ m³/s per meter roof width. Usually gap heights of s ► 20mm are realized, and the efficiency of the ridge vents will appreciably influence the venting efficiency.

The flow in the venting space is caused by wind induced pressure differences between the entrance opening at the eave and the exit opening at the ridge and/or by buoyancy forces. Buoyancy will occur if the temperature of the air in the venting space is increased and hence the density decreased. The pressure difference due to thermal buoyancy is given by

$$\Delta p = g\, H\, (\varrho_a - \varrho_i)$$

with H = vertical dimension of the roof surface, ϱ_a = density of the ambient air and ϱ_i = density of the air in the venting space.

The wind induced pressure difference depends on the wind stagnation pressure at roof height and on the pressure distribution due to the building flow field. For the median wind speed of about 4m/s the wind induced pressure difference for a roof of pitch angle 30° is approximately Δp = 3 Pa.[10] The buoyancy induced pressure difference depends mainly on the temperatures of the ambient air and of the air in the venting space. Figure 14 shows the buoyancy induced pressure difference versus venting space temperature for an ambient temperature ϱ_a = 0°C (winter) and ϱ_a = 20°C (summer). The buoyancy induced pressure difference is roughly of the same order of magnitude as the wind induced pressure difference. The air speed in the venting space is typically of the order of 0.3 m/s.[11,12]

Efficiency of Ridge Vents

The German Standard DIN 4108, Part 3 contains information concerning minimum cross section areas of entrance and exit openings and of the venting spaces. For roof pitch angles larger than 10°, the entrance areas at the eave have to be at least 0.2 percent of the corresponding roof area or at least 0.02m² per meter eave length. The cross section area of the ridge openings has to be at least 0.5 percent of the total roof area. Prescribing only geometric cross section areas may be misleading. From an aerodynamic point of view, the specification of aerodynamic effective areas would be of advantage. Such information would take into account the efficiency of the vent openings.

There is no code of practice or standard in Europe describing a method to measure the aerodynamic efficiency of ridge or tile vents. However, the problem at hand is similar to the evaluation of the aerodynamic efficiency of smoke vents.[13] This guideline has been used for testing ridge vents. The aerodynamic efficiency has been tested without and with side wind.

Without side wind, the flow through the ridge vent is equivalent to the flow discharging from a reservoir. The efficiency of a ridge vent may thus be specified by a discharge coefficient giving the aerodynamic effective area related to the geometrically free area at the ridge:

$$c_v = A_w / A_g$$

with A_w = aerodynamic effective area and A_g = geometric area of the ridge opening = area between the top battens.

With side wind, the efficiency of ridge vents may be specified by the characteristic curve of the vents.[11] The local flow field at the ridge depends on the shape of the ridge vent, the shape of the tiles and on the building flow field. The main influence parameter for the building flow field is the roof pitch angle (see Figure 3).

A great number of different ridge vents have been tested by WSP Consulting Engineers in the medium speed section of the industrial aerodynamics wind tunnel in their research and development laboratory. The cross section area is 2.2m X 1.5m, the max wind speed in the empty test section U_{max} = 24 m/s. A full scale roof section is fitted in such a way that the pressure distribution near the ridge agrees with the pressure distribution obtained in scale model testing for a building model with a roof pitch angle of 30°. Figure 15 shows schematically the test set-up. The vertical axis of the test specimen is inclined relative to the vertical axis of the test section in order to achieve a realistic pressure distribution near the ridge. The pressure distribution measured along the center line of the test specimen and the equivalent pressure distribution obtained in model scale testing are also shown in Figure 14. The pressure in the attic and thus the volume flow through the ridge vent may be varied by means of a radial fan.

The discharge coefficients without side wind range from c_{vo} = 0.1 to c_{vo} = 0.3 for the various ridge vents tested. Thus, the venting may be greatly influenced by the aerodynamic efficiency of the ridge vents. A similar variation in aerodynamic efficiency is apparent from the various characteristic curves obtained (see Figure 16). Since only relative performances have been considered in the comparison tests, the local flow velocity v_D and the local stagnation pressure q_D near the ridge have been used as reference values.

Snow Safety

In cold climates, snow may be driven by wind through the ridge vent into the attic, possibly causing water damage. No information could be found in the literature concerning snow flake size related to the snow density. However, the snow flake size is an important parameter in the prediction of snow penetration. Very light snow, consisting of small snow flakes, seems to be critical for snow penetration. Therefore, very finely ground wheat bran was used as snow substitute for the snow penetration tests. Again, only a comparison test between the various ridge vents was targeted. All tests were conducted with the same amount of snow substitute distributed evenly on the windward side of the tunnel floor. The amount of bran collected in the attic space after the test is a measure of the expected snow penetration. The differences in snow safety of the various vents tested were remarkably high. The worst ridge vent collected about 10 times as much snow substitute as snow collected by the best one. It should be noted that good wind safety does not necessarily mean a reduced aerodynamic efficiency of ridge vents. Well designed ridge vents have a good aerodynamic efficiency, and at the same time, a small risk of snow penetration.

REFERENCES

[1] Kramer, C., Gerhardt, H.J and Kuster, H.W, "The wind loading mechanism of roofing elements," *Journal of Industrial Aerodynmics*, 4 pp. 415-427, 1979.

[2] Gerhardt, H.J. and Kramer, C., "Wind loads on wind permeable facades," Proc., 5th Coll. on Ind. Aerodynamics, Aachen, Part 1, pp. 39-58, 1982.

[3] Gerhardt, H.J., Bofah, K.K. and Kramer, C., "Lagesicherheit lose verlegter Warmedammplatten auf Flachdachern," Bautechnik 67, Heft 2, 55-60, 1990.

[4] Chien, N., et al., "Wind tunnel studies of pressure distribution of elementary building forms," Iowa Institute of Hydraulic Research, State University of Iowa, 1951.

[5] Kramer, C., Gerhardt, H.J. and Scherer, S., "Wind pressures on block-type buildings," *Journal of Industrial Aerodynamics*, 4, pp. 229-242, 1979.

[6] Kramer, C., Gerhardt, H.J. and Kuster, H.W., "Wind loads on surfaces of low rise buildings," Proc., 4th Coll. on Industrial Aerodynamics, Aachen, Part 1, pp. 33-50, 1980.

[7] Kramer, C. and Gerhardt, H.J., "Wind loads on permeable roofing systems," *Journal of Wind Engineering and Industrial Aerodynamics*, 13, pp. 347-358, 1983.

[8] Gerhardt, H.J. and Kramer, C., "Windlasten auf Dachern großer niedriger Industriebauten" (will be published in the near future).

[9] Hazelwood, R.A., "The interaction of the principal wind forces on the roof tiles," Proc., 4th Coll. on Industrial Aerodynamics, Aachen, Part 1, pp. 119-130, 1980.

[10] Gerhardt, H.J., "Windeinwirkung an belufteten Dach- und Wandkonstruktionen, Seminar Warme- und Feuchteschutz belufteter Dach- und Wandkonstruktionen," Haus der Technik, Essen, 1987.

[11] Gerhardt, H.J., "Firstlufter im Test," Das Dachdeckerhandwerk 1/89, 18-24.

[12] Liersch, K., "Beluftete Dach- und Wandkonstruktionen," Band 3: Dacher, Bauverlag, 1986.

[13] DIN 18 232 Part 3.

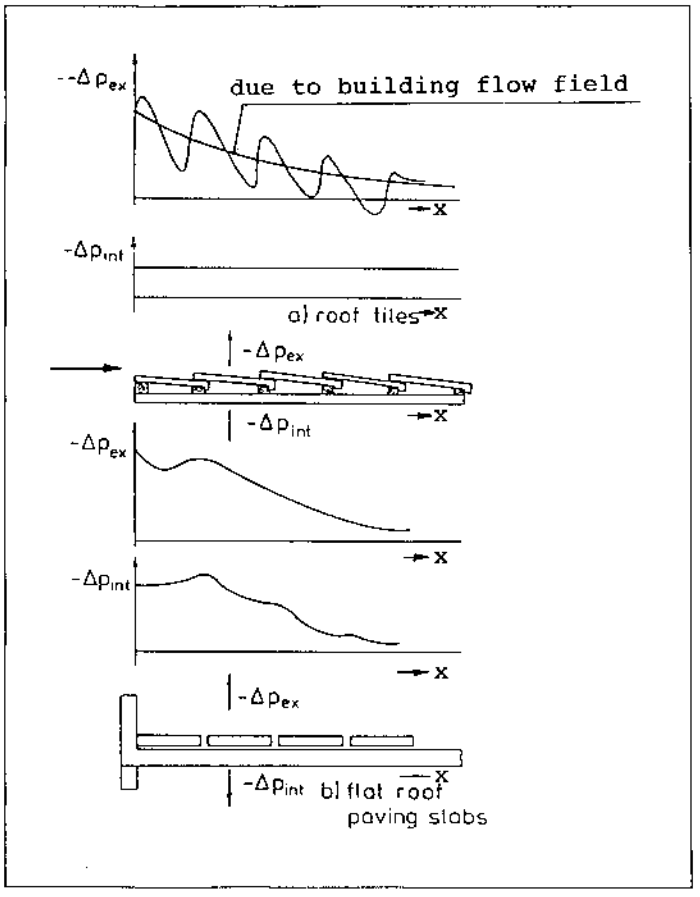

Figure 1

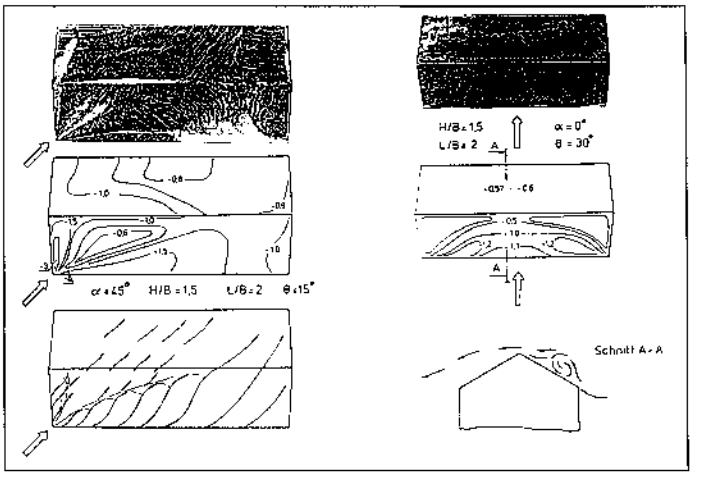

Figure 2

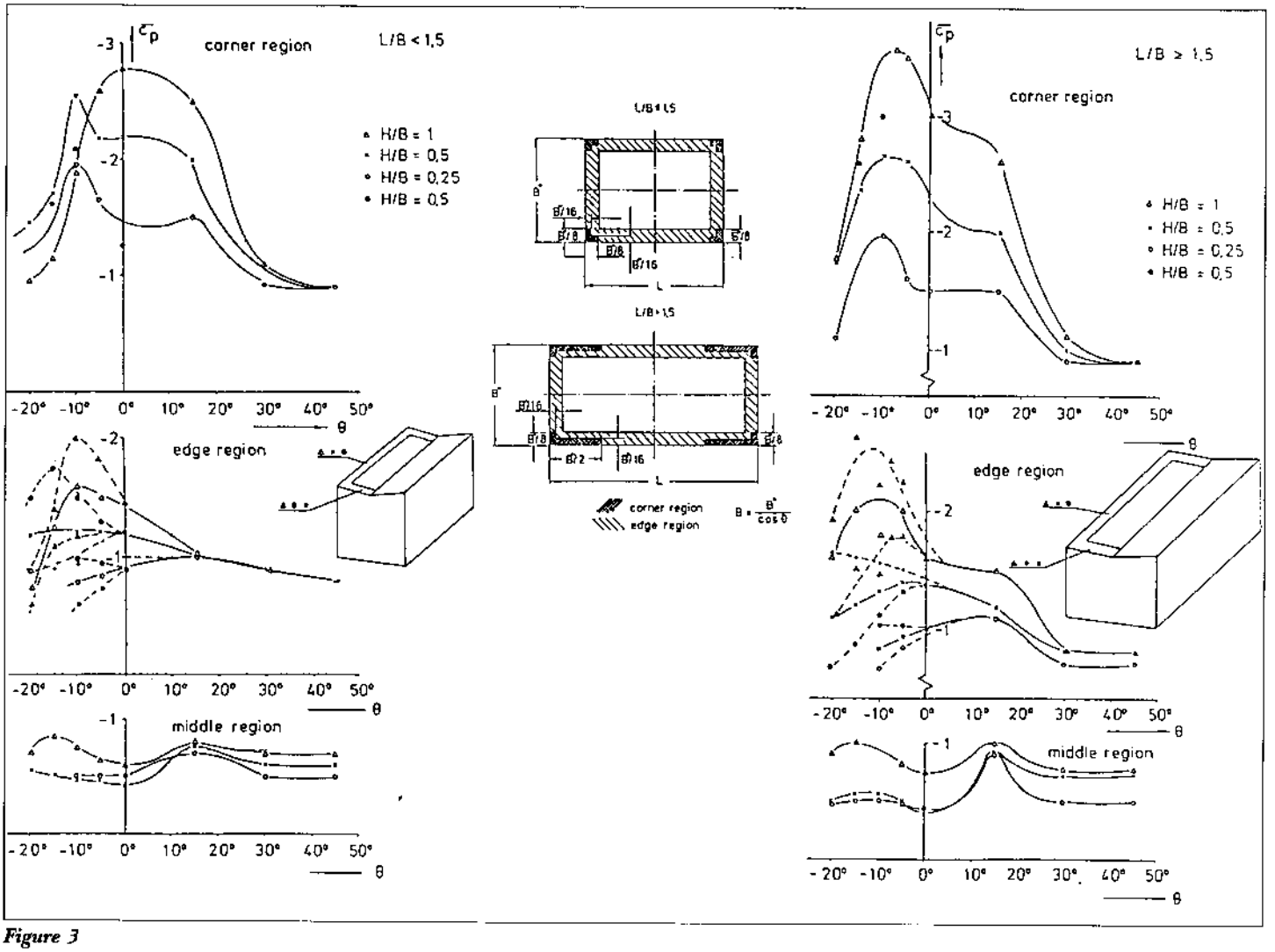
corner region
L/B < 1,5
H/B = 1
H/B = 0,5
H/B = 0,25
H/B = 0,5
edge region
middle region
L/B ≥ 1,5
corner region
edge region

Figure 3

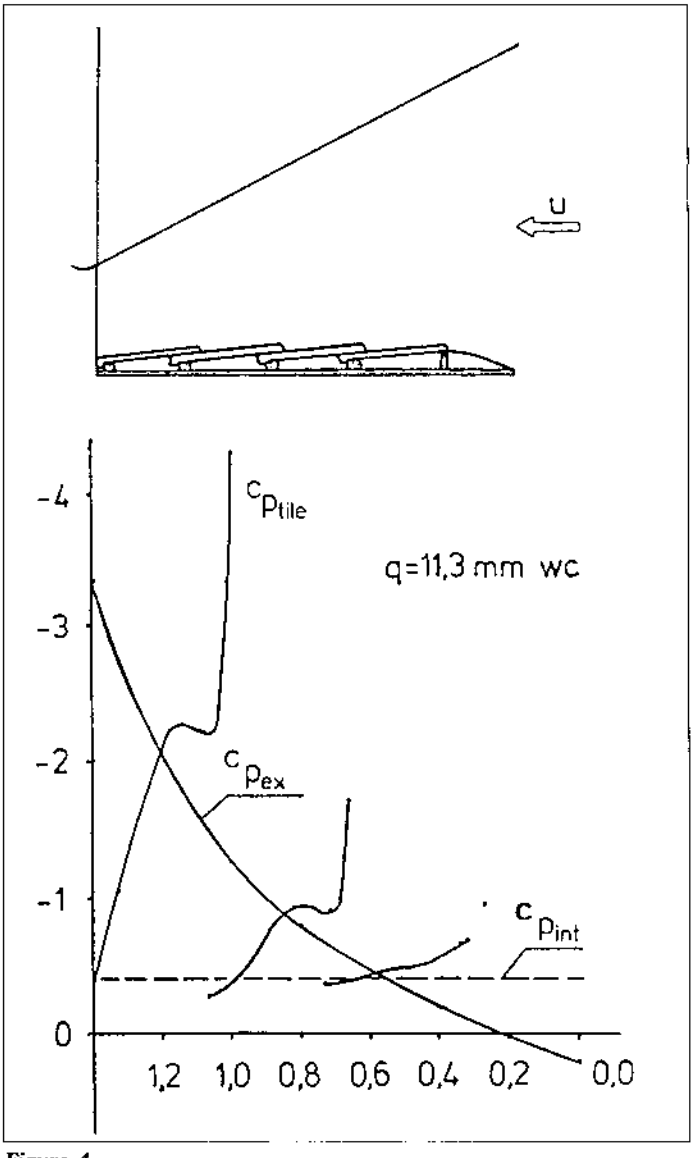

Figure 4

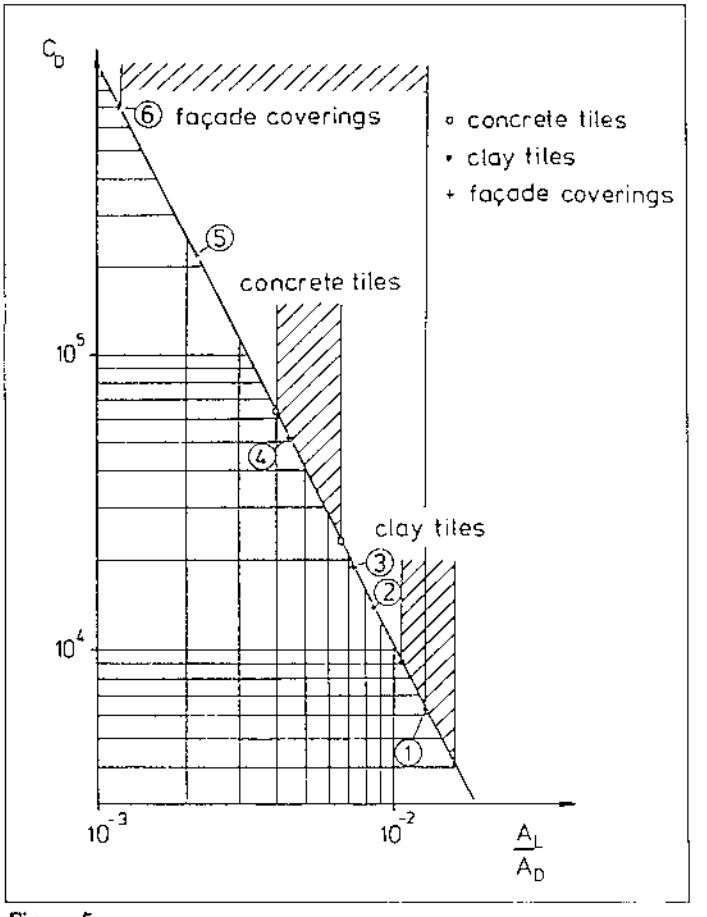

Figure 5

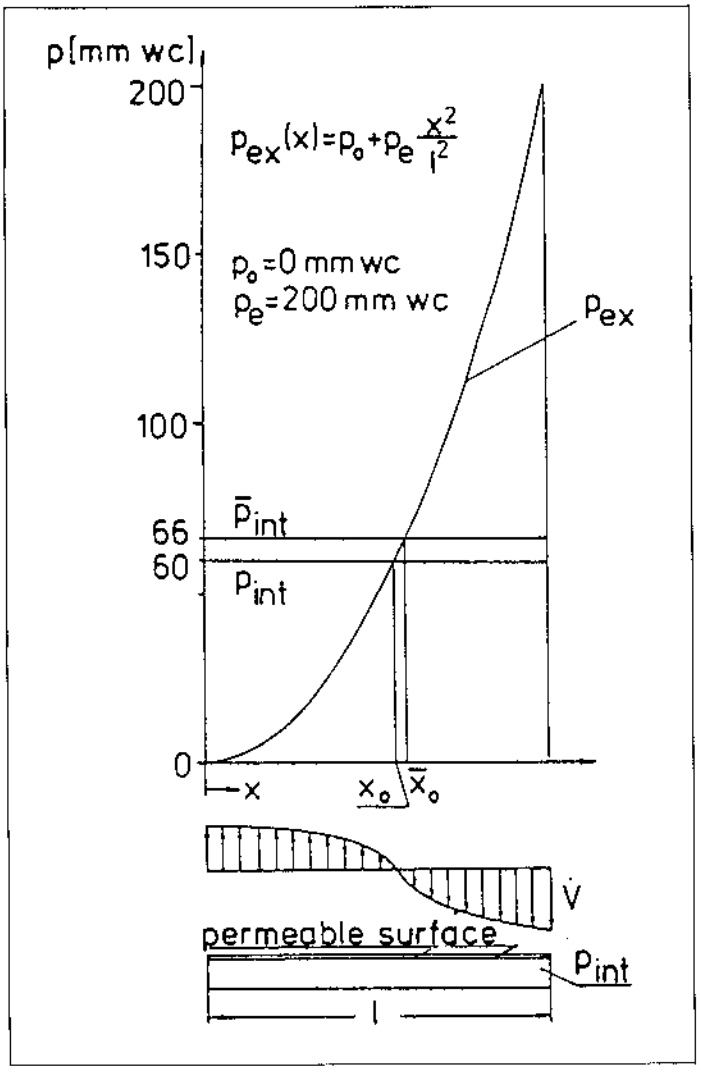

Figure 6

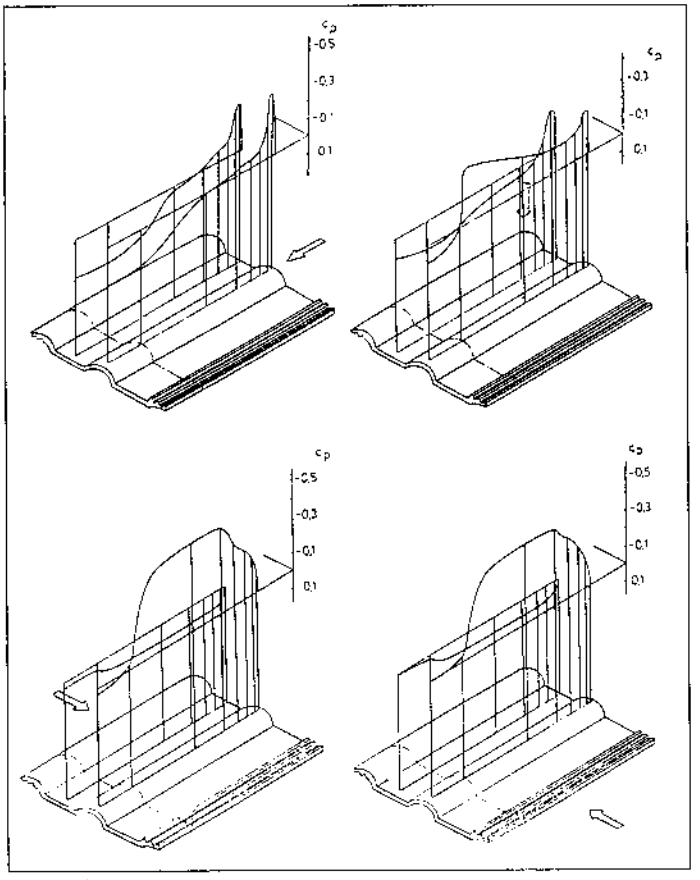

Figure 7

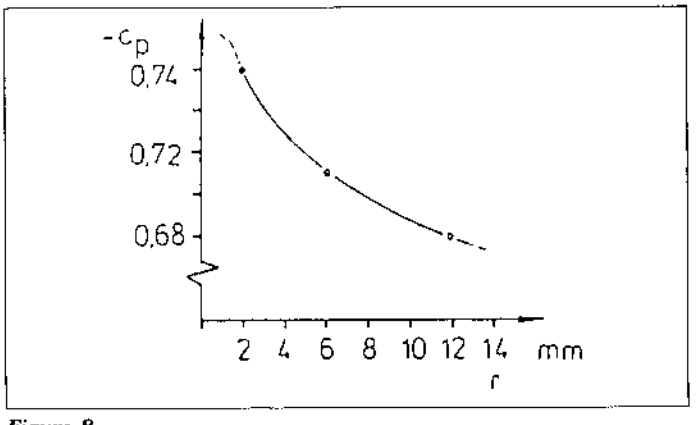

Figure 8

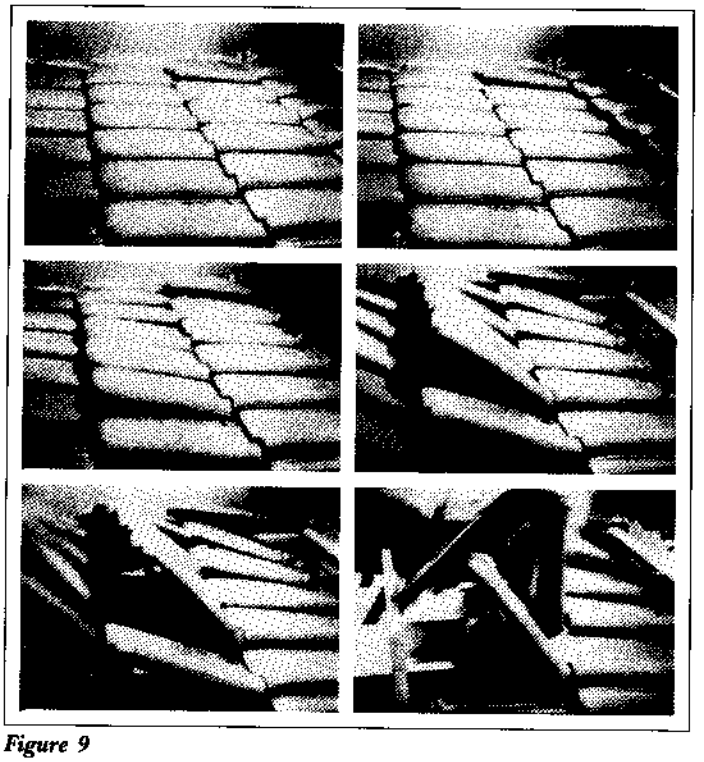

Figure 9

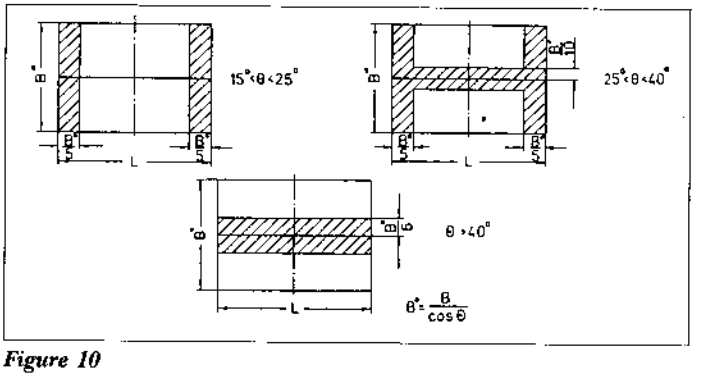

Figure 10

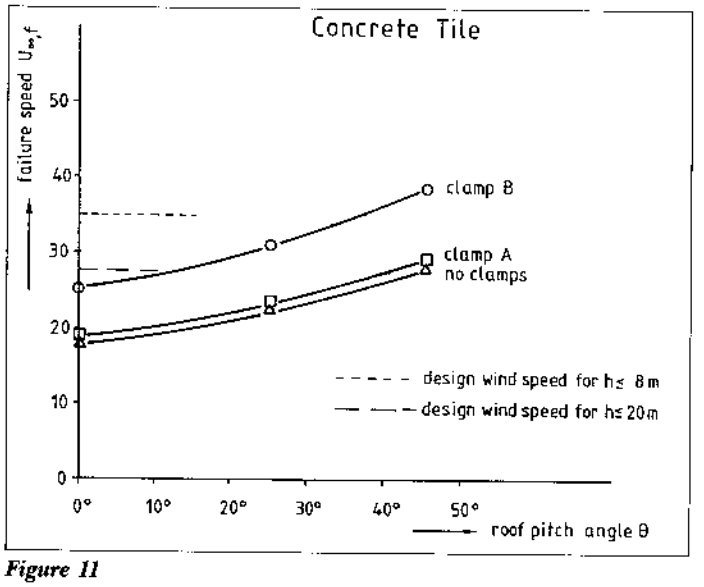

Figure 11

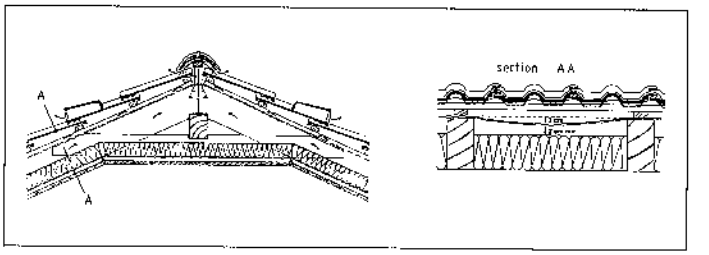

Figure 12

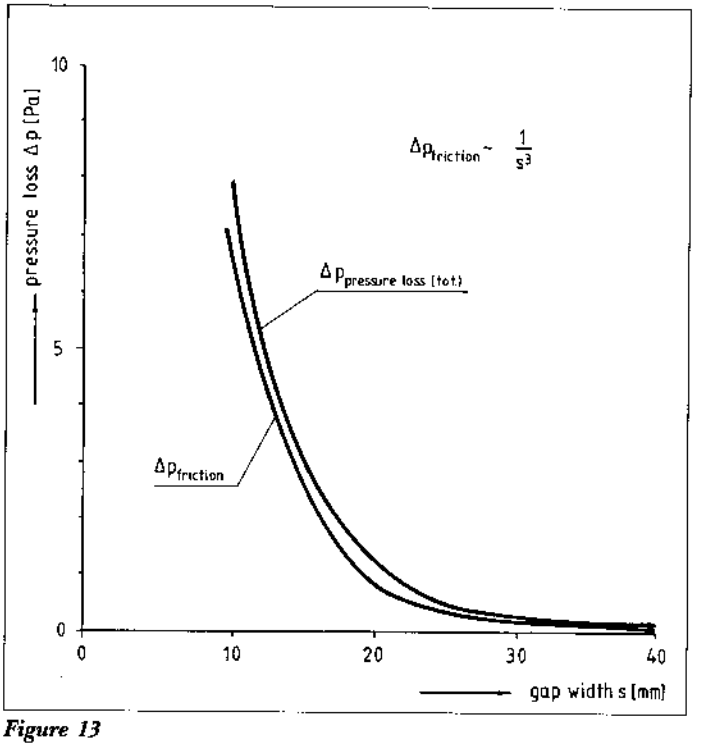

Figure 13

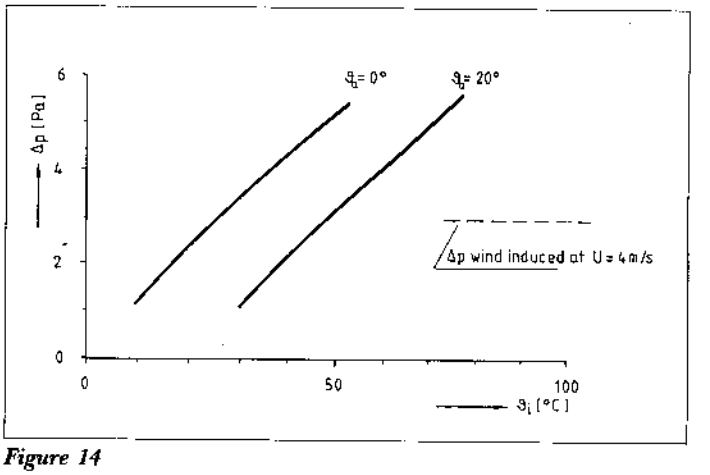

Figure 14

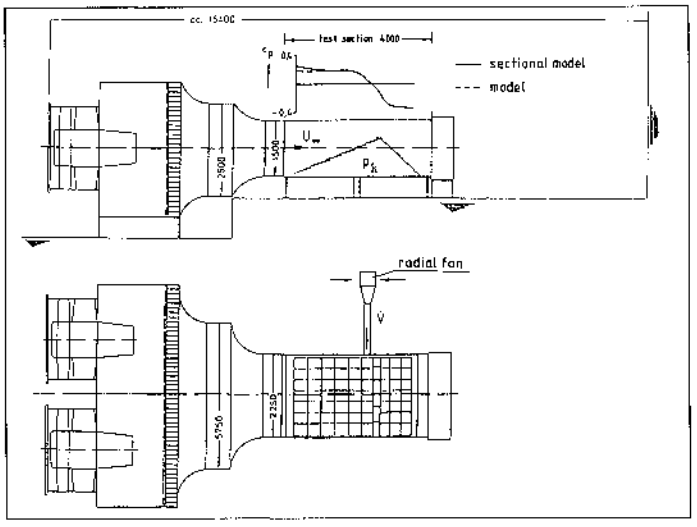

Figure 15

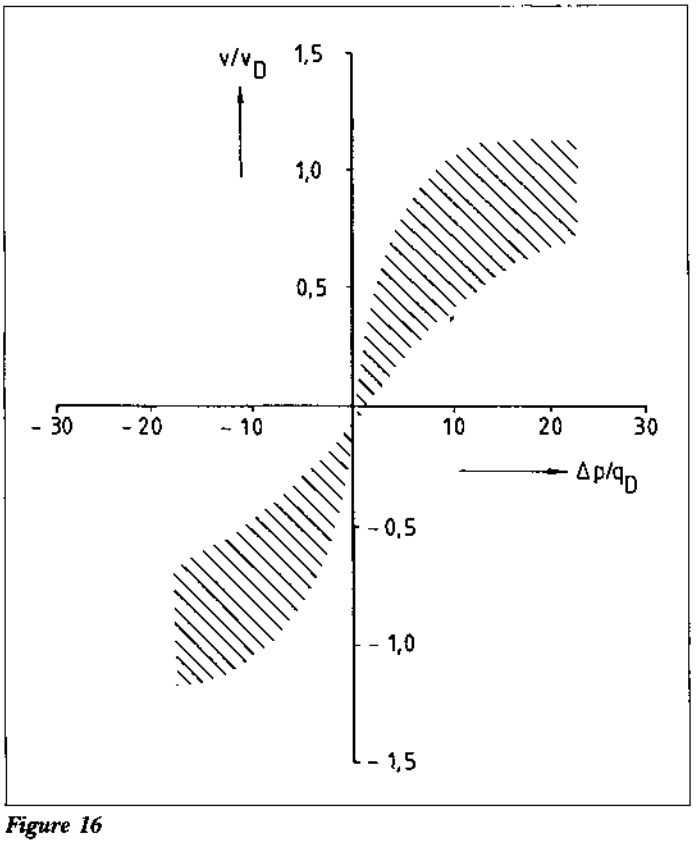

Figure 16